Axial Bearing Capacity of Composite-Sectioned Square Concrete-Filled Steel Tube (Css-Cfst) Columns Stub Reinforced by Circular Steel Tube

Weihua WANG *, [1, 2], Wei ZHANG [1], Qingrong DING [1], Yang BAI [1], Yuye XU [1], Qingwen YANG [1]

[1] College of Civil Engineering, Huaqiao University, Xiamen 361021, China

[2] State Key Laboratory of Subtropical Building Science, Guangzhou 510640, China

***Abstract* — This paper presents the analysis of calculation methods on the bearing capacity of composite-sectioned square concrete-filled steel tube (CSS-CFST) columns under axial compression. Comparison between the calculation results and measured data was conducted with 27 CSS-CFST stub column specimens. The average value or standard deviation of the calculation and tested axial ultimate strength were found overestimated or underestimated. Based on the ABAQUS software, the nonlinear finite element model of CSS-CFST columns was established, and the nonlinear model was validated by experimental results. A revised simplified method for the axial ultimate strength of CSS-CFST columns was proposed herein, according to the axial mechanical behavior analysis by the validated nonlinear FEA model. A good agreement was found between the predicted results and measured data, which could be referred in the further research on the mechanical behavior of the CSS-CFST columns or for the application in constructions.**

Keywords - Composite-sectioned; Concrete-filled steel tube (CFST); Axial compression; Bearing capacity; Simplified calculation method; Finite element model (FEM); Analysis.

I. INTRODUCTION

Following with the fast development of economy and society, concrete-filled steel tube structure was more and more used in super high-rise buildings, and the safety requirement of structures was accordingly getting higher. Questions, such as, high diameter-thickness, high shrinkage of large volume concrete, safety requirement when outside steel tube suffered terror attack, fire or accident impact etc, could be well solved when the normal CFST column was replaced by the composite-sectioned concrete-filled steel tube (CS-CFST) columns [1]. Section types of composite-sectioned columns were illustrated in Fig. (1). Performance of composite-sectioned square concrete-filled steel tube (CSS-CFST) columns reinforced by circular steel tube occupies characteristics of both square CFST columns and circular CFST columns, for example, high bending stiffness, good confinement effect and excellent ductility etc. Several advantages of using CS-CFST columns could also be explained as: (1) Good confinement effect of circular steel tube to core concrete could play full role to improve the bearing capacity and seismic performance of supporting columns, where the axial load was very high or the structure column was especially important. (2) Corrosion of circular steel tube could be well prevented by the protection of concrete, and the durability, fire resistance performance were both improved, as well as the residual capacity after the local buckling of the square steel tube under compression loading. (3) When suffered earthquake or accident terror attack etc, square steel tube may be unloaded from high compression due to local buckling, welding crack etc, and the external concrete could also be crashed, whilst internal circular steel tube and concrete can resist most of the axial load, improve the residual strength of composite columns and prevent structures from local or progressive collapse.

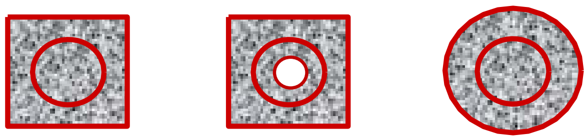

(a) Square section (b) Hollow section (a) Circular section

Figure 1. Section types of CS-CFST columns

There has been lots of research on the axial mechanical behaviour of CS-CFST columns. Zhang Chunmei et al [2, 3] conducted analysis of the effective parameters on the axial ultimate strength of composite-sectioned circular CFST columns reinforced by circular steel tube, and in the purpose of excellent composite effect of CFST columns, a diameter ratio of 0.7~0.8 was suggested for the internal and external circular steel tube. Ref. [4~10] carried out series of experimental test on the axial performance of CS-CFST columns, among which CSS-CFST columns reinforced by circular steel tube (as shown in Fig. (1) (a)) were studied by [4~8], in addition, research on hollow CSS-CFST reinforced by circular steel tube (as shown in Fig. 1(b)) were conducted by [9~10]. Zhang Zhiquan and Zhang Yufen [11~14] proposed a simplified calculation method on the axial ultimate strength of CS-CFST columns using unified theory. According to the yield condition of internal circular steel tube and limit equilibrium, Chen Jianwei et al [15] discussed the simplified calculation methods on the axial bearing capacity of CSS-CFST columns; however, only the confinement effect of internal circular steel tube

DOI 10.5013/IJSSST.a.17.38.06

ISSN: 1473-804x online, 1473-8031 print

was included, the predicted axial ultimate strength was conservative. After then Chen et al [16] start to convert the different concrete strength inside and outside the circular steel tube, and proposed a revised unified method to predict the axial ultimate strength of CSS-CFST columns. Wang Weihua et al [17, 18] conducted nonlinear FE analysis on the axial ultimate strength of CSS-CFST columns, and a good agreement was found between the simulation and measured data.

Research results on the axial ultimate strength of CSS-CFST columns were summarized in this paper, and comparison between the simplified calculation methods was also carried out. The nonlinear FEA model of CSS-CFST columns was established, and the FEA model was validated by test results. Based on the analysis results of FE model, a revised simplified method on the axial ultimate strength of CSS-CFST columns was proposed.

Forced by the conveying pressure, the solid-plug in the passageway 13 enters in to a cavity 14. Due to the different velocity between the rotary part I and II, the plastic resinous material in the cavity 14, has to suffer the shearing force. This phase is called the shearing element. In the shearing element, the plastic resinous material completes further plastication and homogenization. According to the Weissenberg effect, the motion direction of the plastic resinous material is from the periphery of the cavity 14 to the center, which is similar to the motion of dish extruders. For further homogenization, the short screw 5 connected to the rotor 1 by a bolt is disposed in the center. At last, the plastic resinous material, which has been homogenized sufficiently, is extruded out through a die 17. We call this phase the homogenization element, just like the conventional extrusion process.

II. EXPERIMENTAL INVESTIGATION

Totally, the experimental research on the axial mechanical behaviour of 27 CSS-CFST columns was conducted by Pei Wanji and Qian Jiaru et al [5, 7], among which 1 specimens was normal square CFST column in contrast. The total dimension of the CSS-CFST columns was 120 mm and 180 mm, respectively. Parameters of experimental specimens in detail were listed in Table 1.

III. SIMPLIFIED CALCULATION METHODS

There were several theory for the prediction of the axial ultimate strength of CS-CFST columns, such as, direct superposition method, superposition method considering confinement effect, unified theory and limit equilibrium theory etc [7~16]. Four calculation methods were extracted for the prediction of the axial bearing capacity of CSS-CFST column, which were descript as follows:

Method (1): neither the confinement effect of circular CFST section nor that of square CFST section was included, the square and circular steel tube were assumed to only contribute axial bearing capacity [7, 13], the equation for prediction the axial bearing capacity of CSS-CFST columns is as follows:

$$N_1 = A_{so} \cdot f_{so} + A_{si} \cdot f_{si} + A_{co} \cdot f_{cko} + A_{ci} \cdot f_{cki} \quad (1)$$

In which, N_1 is the predicted axial ultimate strength of CSS-CFST columns using method (1), f_{so} is yield strength of square steel tube, f_{si} is yield strength of circular steel tube, f_{cko} is characteristic compressive strength of concrete outside circular steel tube, f_{cki} is characteristic compressive strength of concrete inside circular steel tube, A_{so} is area of square steel tube, A_{co} is area of concrete outside circular steel tube, A_{si} is area of circular steel tube, A_{ci} is area of concrete inside circular steel tube.

Method (2): only the confinement effect of circular section was considered, however, the square steel tube contributes to the axial bearing capacity. The calculation equation is as follows:

$$N_2 = A_{so} f_{so} + A_{co} f_{cko} + N_{a2} \quad (2)$$

In which, N_2 is the predicted axial ultimate strength of CSS-CFST columns using method (2), and N_{a2} is the axial ultimate strength of the circular CFST section with confinement effect:

$$N_{a2} = (1.14 + 1.02\xi_2) \cdot f_{cki} \cdot A_{sci} \quad (2a)$$

Where, ξ_2 is the confinement effect coefficient of the circular CFST section, $\xi_2 = f_{si} A_{si} / (f_{cki} A_{ci})$, f_{cki} is the characteristic compressive strength of concrete inside circular steel tube, the value of f_{cki} could be determined as [19-21].

Method (3): the confinement effect of both circular CFST section and square CFST section was considered, whilst, the confinement effect of square CFST section was the confinement of square steel tube to the concrete outside the circular steel tube:

$$N_3 = N_{a1} + N_{a2} \quad (3)$$

In which, N_3 is the predicted axial ultimate strength of CSS-CFST columns using method (3), and N_{a2} is the same as in method (e), N_{a1} is the axial ultimate strength of the square CFST section with confinement effect:

$$N_{a1} = (1.18 + 0.85\xi_1) \cdot f_{cko} \cdot A_{sco} \quad (3a)$$

Where, ξ_1 is the confinement effect coefficient of the square CFST section, $\xi_1 = f_{so} A_{so} / (f_{cko} A_{co})$, f_{cko} is the characteristic compressive strength of concrete outside circular steel tube, the value of f_{cko} could be determined as [19-21].

Method (4): the confinement effective coefficients of square and circular CFST section were converted into the coefficient of equivalent composite confinement effect:

$$N_4 = (1.212 + \alpha \cdot \xi_4 + \beta \cdot \xi_4^2) \cdot A \cdot f_{cc} \quad (4)$$

In which, N_4 is the predicted axial ultimate strength of CSS-CFST columns using method (4), A is the total area of composite section, □4 is the coefficient of equivalent composite confinement effect, $\xi_4 = (k_o A_{so} f_{so} + k_i A_{si} f_{si}) / (A_c f_{cc})$, k_o and k_i were the calculation coefficient for external and internal steel tubes, respectively, and the value was determined in Ref. [12~14], α and β were parameters for the contribution of steel and concrete, respectively:

$$f_{cc} = \frac{A_{co} f_{co} + A_{ci} f_{ci}}{A_{co} + A_{ci}} \quad (4a)$$

$$f_{ss} = \frac{A_{so}f_{so} + A_{si}f_{si}}{A_{so} + A_{si}} \tag{4b}$$

$$\alpha = 0.1759 f_{ss} / 235 + 0.974 \tag{4c}$$

$$\beta = -0.1038 f_{cc} / 20 + 0.0309 \tag{4d}$$

The predicted axial ultimate strength of CSS-CFST columns using method (1~4) was listed in Table 2, as well as the measured results of the test specimens. Due to the advantage of confinement effect of steel tube to concrete, the predicted axial ultimate strength of CSS-CFST columns of method (1)~(3) increase in proper order. However, the real axial bearing capacity of square steel tube was less than the product of the area of square steel tube (A_{so}) and its yield strength (f_{so}), because when the width-thickness ratio of square steel tube was high, local buckling would occur before the external steel tube yield, reducing the axial bearing capacity of the square steel tube. For all that, most

TABLE 1 PARAMETERS SUMMARY OF CSS-CFST TEST SPECIMENS

No.	$B_1 \times t_1$ /mm	$D_2 \times t_2$ /mm	L /mm	f_{so} /MPa	f_{si} /MPa	f_{cu1} /MPa	f_{u2} /MPa	Ref.
1	120×2.60	-	360	407.5	-	35.2	35.2	Ref.5
2	120×2.60	58.5×1.4	360	407.5	352.5	35.2	35.2	Ref.5
3	120×2.60	74×0.9	360	407.5	680	35.2	35.2	Ref.5
4	120×2.60	83×0.9	360	407.5	597	35.2	35.2	Ref.5
5	180×3.62	89×2.6	600	348	314	105.7	87.5	Ref.7
6	180×3.62	89×3.32	600	348	324	105.7	87.5	Ref.7
7	180×3.62	114×4.56	600	348	322	105.7	87.5	Ref.7
8	180×3.62	140×2.84	600	348	345	105.7	87.5	Ref.7
9	180×5.4	89×2.6	600	338	314	105.7	87.5	Ref.7
10	180×5.4	89×3.32	600	338	324	105.7	87.5	Ref.7
11	180×5.4	114×3.35	600	338	328	105.7	87.5	Ref.7
12	180×5.4	114×4.56	600	338	322	105.7	87.5	Ref.7
13	180×5.4	140×2.84	600	338	345	105.7	87.5	Ref.7
14	180×5.4	140×3.97	600	338	308	105.7	87.5	Ref.7
15	180×3.62	89×2.6	600	348	314	87.5	105.7	Ref.7
16	180×3.62	114×3.35	600	348	328	87.5	105.7	Ref.7
17	180×5.4	89×2.6	600	338	314	87.5	105.7	Ref.7
18	180×5.4	114×3.35	600	338	328	87.5	105.7	Ref.7
19	180×5.4	140×3.97	600	338	308	87.5	105.7	Ref.7
20	180×5.4	89×3.32	600	338	324	87.5	105.7	Ref.7
21	180×3.62	89×2.6	600	348	314	87.5	87.5	Ref.7
22	180×3.62	114×3.35	600	348	328	87.5	87.5	Ref.7
23	180×3.62	140×3.97	600	348	308	87.5	87.5	Ref.7
24	180×5.40	89×2.60	600	338	314	87.5	87.5	Ref.7
25	180×5.40	114×3.35	600	338	328	87.5	87.5	Ref.7
26	180×5.40	140×3.97	600	338	308	87.5	87.5	Ref.7
27	180×5.40	89×3.32	600	338	324	87.5	87.5	Ref.7

TABLE 2 AXIAL BEARING CAPACITY COMPARISON OF THE CSS-CFST SPECIMENS BETWEEN THE PREDICTED AND MEASURED RESULTS

No.	Test	Method (1)		Method (2)		Method (3)		Method (4)		Method (5)	
	N_{ue}/KN	N_1/KN	N_1/N_{ue}	N_2/KN	N_2/N_{ue}	N_3/KN	N_3/N_{ue}	N_4/KN	N_4/N_{ue}	N_5/KN	N_5/N_{ue}
1	880	804	0.913	804	0.913	858	0.975	873	0.994	858	0.975
2	980	886	0.904	912	0.931	965	0.984	887	0.905	939	0.958
3	1040	939	0.903	968	0.931	1023	0.984	939	0.903	983	0.945
4	1080	937	0.867	969	0.897	1027	0.951	937	0.868	983	0.911
5	3643	3249	0.892	3380	0.928	3883	1.066	3381	0.928	3778	1.037
6	3583	3305	0.923	3470	0.969	3972	1.109	3452	0.963	3855	1.076
7	3820	3421	0.896	3710	0.971	4174	1.093	3693	0.967	3975	1.040
8	3940	3284	0.834	3539	0.898	3967	1.007	3644	0.925	3733	0.948
9	3865	3528	0.913	3659	0.947	4294	1.111	3676	0.951	4190	1.084
10	3947	3584	0.908	3749	0.950	4384	1.111	3743	0.948	4266	1.081
11	4045	3602	0.890	3820	0.944	4440	1.098	3862	0.955	4266	1.055
12	4121	3699	0.898	3989	0.968	4608	1.118	3978	0.965	4409	1.070
13	4251	3563	0.838	3818	0.898	4453	1.048	3948	0.929	4220	0.993
14	4258	3634	0.853	3949	0.927	4585	1.077	4040	0.949	4332	1.017
15	3355	2987	0.890	3141	0.936	3538	1.054	4162	1.241	3418	1.019
16	3686	3170	0.860	3426	0.930	3795	1.030	4340	1.177	3596	0.976
17	3814	3285	0.861	3439	0.902	3951	1.036	4550	1.193	3832	1.005
18	4043	3468	0.858	3724	0.921	4232	1.047	4703	1.163	4032	0.997
19	4428	3643	0.823	4015	0.907	4552	1.028	4795	1.083	4260	0.962
20	3855	3338	0.866	3529	0.915	4041	1.048	4640	1.204	3908	1.014
21	3198	2906	0.909	3038	0.950	3435	1.074	3527	1.103	3330	1.041
22	3415	3038	0.890	3257	0.954	3626	1.062	3714	1.088	3452	1.011
23	4120	3146	0.764	3461	0.840	3808	0.924	3866	0.938	3554	0.863
24	4021	3204	0.797	3335	0.829	3848	0.957	3868	0.962	3744	0.931
25	4165	3336	0.801	3555	0.853	4062	0.975	4043	0.971	3888	0.934
26	4436	3444	0.776	3759	0.847	4296	0.969	4185	0.943	4043	0.911
27	3900	3261	0.836	3425	0.878	3938	1.010	3946	1.012	3820	0.980
Average value			0.865		0.916		1.036		1.008		0.994
Standard deviation			0.043		0.038		0.055		0.104		0.057

Note: N_{ue} is the measured axial bearing capacity of the CSS-CFST specimens listed in Table 1, N_1、N_2、N_3、N_4 is the predicted axial bearing capacity of the CSS-CFST specimens corresponding to the method (1)~(4), respectively, N_5 is the predicted axial bearing capacity of the CSS-CFST specimens corresponding to the method (5), which would be discussed in the following section 5.

were less than the measured ones, especially for those of the method (1), the predicted bearing capacity of the CSS-CFST specimens was 10~20% less than the test results. Though the confinement effect of square steel tube and circular steel tube and the effect of local buckling of square steel tube were considered in the method (3) [19], the predict results of the CSS-CFST specimens was about 8~10% higher than the measured results. Compared with the former three method, the average predicted results was close to the measured ones, but the standard deviation of the predicted-measured bearing capacity ratio (N_{up}/N_{ue}) was meetly high, the highest tolerance was about 24%.

The standard deviation of N_{up}/N_{ue} was 0.043, 0.038, 0.055 and 0.104, respectively. It could be found that the standard deviation of the method (2) was the smallest, whilst that of the method (4) was the highest of all.

The ratio of the predicted and measured results was illustrated in Fig.(2). Obviously, the predicted axial ultimate strength from the method (1) and (2) was lower than the test results, whilst those from the method (3) were higher than the measured axial bearing capacity. Though the average of the predicted results was 1.008, the axial ultimate strength of some CSS-CFST specimens was unreasonably overestimated by the method (4), as shown in Fig. 2.

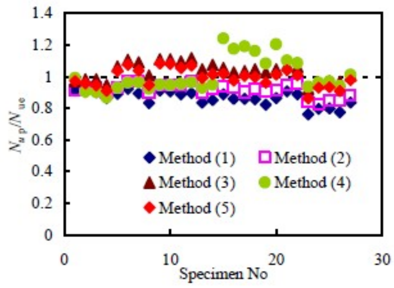

Figure 2. Ratio between the predicted and measured results of CSS-CFST specimens

IV. FINITE ELEMENT ANALYSIS

A. Material Model

The adopted material model of steel and concrete in the FEA model was according to the method in Ref. [19]: a five-stage model and a bilinear model was proposed for the low-carbon or lean-alloy steel and high-strength steel, respectively; meanwhile the steel-to-concrete confinement effect and concrete strength was included the stress-strain relationship of core concrete. The above material has been validated by a lot of test results, and the equation for the stress-strain relationship of concrete is as follows:

$$y=\begin{cases} 2\cdot x-x^2 & (x\le 1) \\ \dfrac{x}{\beta\cdot(x-1)^{\eta}+x} & (x>1) \end{cases} \qquad (5)$$

In which, $x=\varepsilon_c/\varepsilon_0$, $y=\sigma_c/f_c$, β and η were calculation coefficients, the calculation method is shown in Ref. [17-19].

B. Finite Element Model

Based on the ABAQUS nonlinear software, the axial compression FEA model of CSS-CFST columns was established, among which, the shell element was used to simulate steel tubes and 3D solid element was used to simulate concrete. Totally, 9 integration points of Simpson integral was set along the thickness of steel tubes. Coulomb friction was selected in the contact relationship between steel tube and concrete. The friction coefficient was 0.6, at the same time, separation was allowed in the normal direction of the interface between steel and concrete [22]. The axial compression FEA model of CSS-CFST columns was shown in Fig. (3).

C. Validation by test

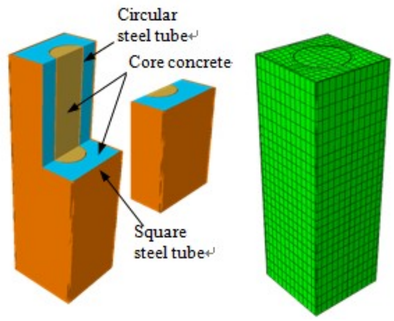

(a) FEA model (b) Element mesh

Figure 3. FEA model of CSS-CFST columns

Based on the above FEA model, a series of simulation and analysis research work was carried out according to the test CSS-CFST column specimens. The predicted and measured axial load (*N*) versus strain (□) relationships of the CSS-CFST specimens were shown in Fig. (4). It could be found that a good agreement was found between the predicted and measured *N*-□□curves. Not only the predicted ultimate strength but the residual strength of the CSS-CFST specimens was close to the measured ones.

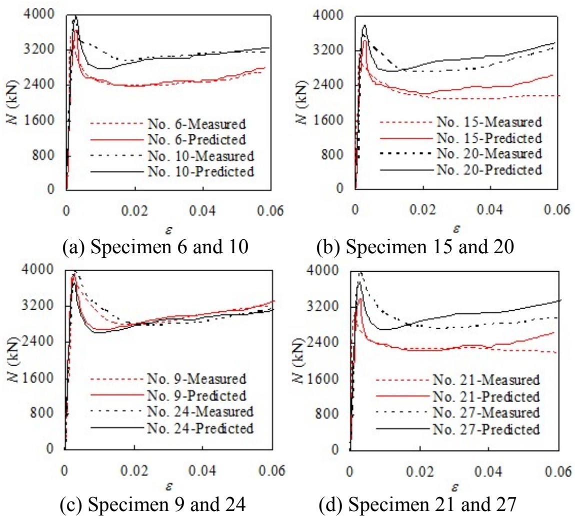

(a) Specimen 6 and 10 (b) Specimen 15 and 20

(c) Specimen 9 and 24 (d) Specimen 21 and 27

Figure 4. Comparison between predicted and measured N-□ curves[7]

All of the CSS-CFST column specimens were simulated in this paper, comparison of the predicted ultimate strength and measured results were illustrated in Fig. (5). It can be seen that the FEM predicted ultimate strength agreed with the test results well, and the tolerance between them was in the range of 10%.

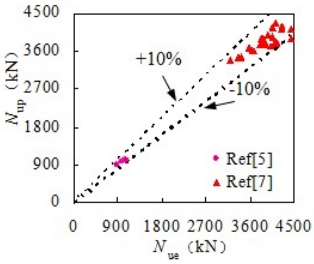

Figure 5. Comparison between predicted and measured results

The typical axial load (N) versus strain (ε) relationship curves and failure mode were shown in Fig. (6) (a) and (b).

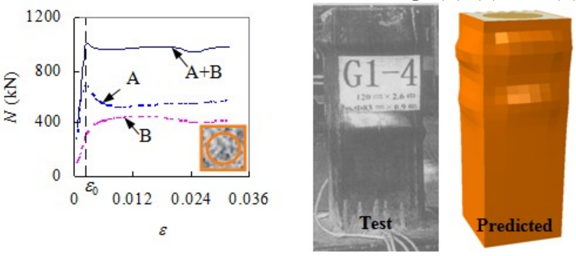

(a) Comparison of N-ε curves (b) Comparison of failure mode[5]

Figure 6. Comparison of N-curves and failure mode between FEM predicted and measured results (Specimen 4)

Curve "A" and "B" represented the axial compression load curves of square and circular CFST sections, and curve "A+B" represented the whole axial compression load (N) versus strain (ε) relationship curve of the CSS-CFST specimens. Characteristics of curve "A" was very similar with curve "A+B", moreover, both of the two curves reached the peak point (bearing capacity) nearly at the same axial strain, as shown in Fig. (6) (a). That's to say, the bearing capacity of square CFST section could be fully developed when the whole CSS-CFST columns reached the axial ultimate strength. At the early stage, curve "A" almost increased linearly with the axial load, at about 80~90% of the axial ultimate strength, the axial strain developed rapidly. After the axial load arrived at the peak point (ultimate strength), it drop down quickly, then the axial load came into a stable stage, that is the residual strength stage. This phenomenon was very similar with those of normal square CFST columns suffered to axial compression [19]. However, it was found that the axial compression strain corresponding to the peak point value of curve "A" was not identical with that of curve "B". At the time of the axial strain (ε_0), the bearing ability of circular CFST section (curve "B") was still in the rising stage. The axial load, token by circular CFST section, was about 82.3% of the ultimate strength of circular CFST section (that is the peak point value of curve "B"). Less axial load loss were found for the CSS-CFST column (curve "A+B") than the square CFST column (curve "B"), the main reason is because of the high residual strength of circular CFST section (curve "B"). This explained why the predicted ultimate strength from method (3) was commonly higher than the measured results, as discussed in Section 3. The predicted typical failure mode also agreed well with that of test specimen, as shown in Fig. (6) (b).

V. REVISION OF SIMPLIFIED CALCULATION METHOD

As discussed above, two partial actions were contained in the ultimate strength of CSS-CFST columns: sectional axial contribution of square CFST section (curve "A") and sectional axial contribution of circular CFST section (curve "B"). Based on the numeric analysis of FEA models, the allocation proportion of bearing axial load by the circular CFST section was about 80~90% of its axial ultimate strength. Among which, comparison on the axial ultimate strength with the measured results was conducted, research results indicated that when the reduction coefficient for the axial ultimate strength of circular CFST section was 0.85, a better agreement could be received between the predicted and measured results, as shown in Table 2. The simplified calculation equation (method (3)) was revised accordingly as method (5):

$$N_5 = N_{a1} + 0.85N_{a2} \tag{5}$$

In which, N_{a1} and N_{a2} were the axial ultimate strength of square and circular CFST section, which were the same as those in method (3).

The predicted axial ultimate strength of the CSS-CFST specimens from method (5) was also listed in Table 2. It could be found that the difference of ratio between the predicted results and the measured axial ultimate strength of most CSS-CFST specimens was within the range of 5%, and the average value and standard deviation of predicted-to-measured axial ultimate ratio were 0.994 and 0.057, respectively. The revised method (5) was proved to be more reasonable than method (3), and the prediction accuracy and standard deviation was acceptable.

VI. CONCLUSIONS

Based on the limited research, the following conclusions may be made:

(1) A research summary on the axial ultimate strength of CSS-CFST columns was presented, several existing calculation methods were compared with test results.

(2) The nonlinear FEA model of CSS-CFST columns subjected to axial compression was validated by test results, and then the compressive contribution of square and circular CFST sections was discussed.

(3) A revised simplified calculation method was proposed according the FE analysis. Reasonably good agreement is obtained between the measured and predicted results. Research results could be referred in the further research or engineering application.

DOI 10.5013/IJSSST.a.17.38.06

ISSN: 1473-804x online, 1473-8031 print

ACKNOWLEDGEMENTS

This research was supported by National Natural Science Foundation of China projects No. 51208217, National Key Technology Support Program of China 2014BAK09B01 (SQ2013BAJY4193), State Key Laboratory of Subtropical Building Science development fund 2014KB26, Project of Natural Science Foundation of Fujian Province 2014J01195, and Promotion Program for Young and Middle-aged Teacher in Science and Technology Research of Huaqiao University. The financial support is highly appreciated.

REFERENCES

[1] X.D. Fang, S.J. Lin, "Axial compressive test of columns with multi barrel tube-confined high performance concrete ," Journal of Building Structures, vol. 35(4), pp. 236-245, 2014. [in Chinese]

[2] M.X. Liu, "Design method of new composite-sectioned concrete-filled steel tubular columns ," Building Structure, vol. 44(4), pp. 39-43, 2014. [in Chinese]

[3] Ch.M. Zhang, Y. Yin, Y. Zhou, "Analysis of factors influencing axial compressive bearing capacity of concrete-filled steel tube column ," Industrial Construction, vol. 34(10), pp. 66-68, 2004. [in Chinese]

[4] K. Uenaka, H. Kitoh, K. Sonoda. "Experimental study on short concrete filled double steel tubular columns under compression ," Kou Kouzou Rombunshuu, vol. 14(53) , pp. 67-75, 2007.

[5] W.J. Pei, "Research on mechanical performance of multibarrel tube-confined concrete columns ," M.S. thesis, Chang'an University, Xi'an, ON, China, 2005. [in Chinese]

[6] Sh..F. Ma, H.X. Guo, J.H. Zhao, X.Y. Wei, "Experimental investigation on multi-barrel tube-confined concrete under eccentric compression , " Industrial Construction, vol. 37(12), pp. 28-30, 2007. [in Chinese]

[7] J.R. Qian, Y. Zhang, X.D. Ji, W-L. Cao, "Test and analysis of axial compressive behaviour of short composite-sectioned high strength concrete filled steel tubular columns ," Journal of Building Structures, vol. 32 (12), pp. 162-169, 2011. [in Chinese]

[8] Y. Zhang, J.R. Qian, X.D. Ji, W.L Cao, "Experimental study on axial compressive strength of concrete filled composite steel tube short columns ," World Earthquake Engineering, vol. 27(3), pp. 40-46, 2011. [in Chinese]

[9] Zh.H. Wang, R. Cheng, "Axial bearing capacity of composite-sectioned square concrete-filled steel tubes ," Journal of Tsinghua University (Science and Technology), vol. 45(12), pp. 1596-1599, 2005. [in Chinese]

[10] R. Cheng, Zh.H. Wang, "The loading capacity and producing method analysis of composite reinforced SCFT column ," Industrial Construction, vol. 36(9), pp. 84-86, 2006. [in Chinese]

[11] Zh.Q. Zhang, Sh.M. Zhao, Y.F. Zhang, T. Wu. "Calculation method of axial bearing capacity of concrete-filled square steel tubular columns reinforced by inner circular steel tube ," Journal of Architecture and Civil Engineering, vol. 26(2), pp. 63-67, 2009. [in Chinese]

[12] Y.F. Zhang, J.H. Zhao, X.W. Li, "On the axial bearing capacity of composite concrete-filled steel tubes based on the unified theory," Journal of Xi'an University of Architecture and Technology, vol. 41 (1), pp. 41-46, 2009. [in Chinese]

[13] Y.F. Zhang, "Study on axial compressive behaviour of the composite CFST and seismic on RC beam-column connections ," Doc. Dissertation, Chang'an University, Xi'an, ON, China, 2010. [in Chinese]

[14] Zh.Q. Zhang, J.H. Zhao, Y.F. Zhang, X.W. Li, "Axial bearing capacity of composite concrete-filled steel tubular columns ," Journal of Chang'an University (Natural Science Edition), vol. 30 (1), pp. 67-70, 2010. [in Chinese]

[15] J.W. Chen, Y.P. Su, H.B. Chen, L. Gao, "Calculation method of axial compressive bearing capacity for composite-sectioned concrete-filled steel tubular columns based on the limit equilibrium theory ," China Civil Engineering Journal, vol. 46 (S1), pp. 106-110, 2013. [in Chinese]

[16] J.W. Chen, Y.P. Su, X. Li, "Contrast and analysis on computational methods of axial compressive bearing capacity for composite-sectioned concrete filled steel tubular columns ," Journal of Fuzhou University (Natural Science Edition), vol. 41(4), pp. 792-795, 2013. [in Chinese]

[17] W.H. Wang, G.H. Yao, Y.Y. Xu, "Influence factor analysis of composite-sectioned concrete-filled steel tube columns reinforced by circular steel tube based on orthogonal experimental ," Journal of Qingdao Technology University, vol. 33(2), pp.16-21, 2012. [in Chinese]

[18] W.H. Wang, G.H. Yao, L.L. Wang, "FE analysis of axial behaviour of composite-sectioned square concrete filled steel tube stub columns reinforced by circular steel tube ," Journal of Beijing University of Technology, vol. 39(6), pp. 99-104, 2013. [in Chinese]

[19] L.H. Han, Concrete-filled structures: theory and experience, Beijing: Science Press, 2007. [in Chinese]

[20] DBJ/T13-51-2010. Technical specification for concrete-filled steel tubular structures, Fuzhou (China): The Department of Housing and Urban-Rural Development of Fujian Province, 2010. [in Chinese]

[21] GB 50010-2010. National standard of China: Code for design of concrete structures, Beijing: China Architecture and Building Press, 2010. [in Chinese]

[22] W.H. Wang, L.H. Han, W. Li, Y.H. Jia. "Behaviour of Concrete-Filled Steel Tubular Stub Columns and Beams using Dune Sand as Part of Fine Aggregate ," Construction and Building Materials, vol. 51(31), pp. 352-363, 2014.